Monolithically Integrated Optical Phase Lock Loop for Microwave Photonics

Katarzyna Balakier, Martyn J. Fice, *Member, IEEE*, Lalitha Ponnampalam, Alwyn J. Seeds, *Fellow, IEEE*, and Cyril C. Renaud, *Member, IEEE*

***Abstract*—We present a review of the critical design aspects of monolithically integrated optical phase lock loops (OPLLs). OPLL design procedures and OPLL parameters are discussed. A technique to evaluate the gain of the closed loop operating system is introduced and experimentally validated for the first time. A dual-OPLL system, when synchronised to an optical frequency comb generator without any prior filtering of the comb lines, allows generation of high spectral purity signals at any desired frequency from several GHz up to THz range. Heterodyne phase locking was achieved at a continuously tuneable offset frequency between 2 and 6 GHz. Thanks to the photonic integration, small dimensions, and custom-made electronics, the propagation delay in the loop was less than 1.8 ns, allowing good phase noise performance with OPLLs based on lasers with linewidths less than a few MHz. The system demonstrates the potential for photonic integration to be applied in various microwave photonics applications where narrow-bandwidth tuneable optical filters with amplification functionality are required.**

***Index Terms*—Microwave generation, microwave photonics, optical mixing, optical phase locked loops (OPLLs), phase noise, photonic integrated circuits, semiconductor lasers.**

I. Introduction

PHOTONIC systems suitable for generation, transmission and processing of microwave signals have been investigated over the last few decades [1], [2]. The ability to transport microwave frequencies over long distances with little penalty in the optical domain was one of the key advantages that led to the development of microwave photonic systems [3], [4].

The key component of many microwave photonic systems is a semiconductor laser, which may have a linewidth in the range of tens of MHz and whose frequency (wavelength) is characterised by a low stability caused by the laser's thermal drift or its mode changes. However, for certain applications a narrow linewidth microwave source with a stable absolute frequency is required, thus phase stabilisation is needed. The phase of a photonic microwave source can be stabilised by controlling the relative phase between two lasers and may be achieved by a number of locking techniques in various photonic system configurations: optical phase lock loop (OPLL) [5], optical injection locking (OIL) [6], and a combination of these two—optical injection phase lock techniques (OIPLL) [7]. Some of the locking techniques rely on the synchronization to an optical comb [8], single frequency reference signal or one of its harmonics [9]. Regardless of the type of reference source applied, OIL has a number of characteristics which prevent it from being easily implemented and broadly applied. These include a narrow and asymmetric stable locking bandwidth as well as instabilities inside the locking range for higher levels of injected optical power. Secondly, OIL is a purely homodyne technique, thus having no potential for continuous tuning of an offset between the slave and the reference laser. The OIPLL seems to be a solution capable of overcoming some of the limitations of the OPLL (narrow linewidth laser and short feedback loop delay) and OIL (narrow stable locking range). The combination of optical injection locking of the semiconductor laser and low speed electronic feedback offers a wide locking bandwidth together with large tracking range [10]. However, the combination of two locking techniques adds complexity to the system, and the issue of offset tuneability remains outstanding. Against this backdrop, the OPLL could be considered a preferable technique as it allows offset phase locking, which thus enables adjustable frequency spacing between the lasers. Such a coherent system could potentially find its use in various applications, including high-sensitivity detection, ultra-high data rate wireless communication and room temperature generation of broadly tuneable THz signals [11]. Moreover, the OPLL has the potential for being applied as an elementary building block in many photonic systems, where active, narrow-bandwidth, high-rejection optical filters are required.

Many of the photonics solutions applied in the microwave frequency domain are based on complex systems which rely mostly on discrete components. As constant improvements in the performance and fabrication yield of photonic integrated circuits is observed [12], there is enough evidence that monolithic photonic integration could offer advantages in terms of a significant reduction in the system footprint, inter-element coupling losses, packaging costs, and system power consumption thanks to the use of a single cooler for multiple functions. Moreover, advances and decreasing fabrication cost in photonic integration have been triggered by the recent availability of numerous generic fabrication platforms [13], thus simplifying the development of advanced integrated photonic systems.

Manuscript received January 15, 2014; revised March 4, 2014; accepted April 1, 2014. Date of publication April 16, 2014; date of current version September 1, 2014. This work was supported by the European Community's Seventh Framework Programme, carried out within the framework of the MITEPHO Initial Training Platform, and the EPSRC and the European Commission through the COTS, PORTRAIT, and IPHOBAC projects.

The authors are with the Department of Electronic and Electrical Engineering, University College London, London, WC1E 7JE, U.K. (e-mail: k.balakier@ucl.ac.uk; m.fice@ucl.ac.uk; l.ponnampalam@ucl.ac.uk; a.seeds@ucl.ac.uk; c.renaud@ucl.ac.uk).

Color versions of one or more of the figures in this paper are available online at http://ieeexplore.ieee.org.

Digital Object Identifier 10.1109/JLT.2014.2317941

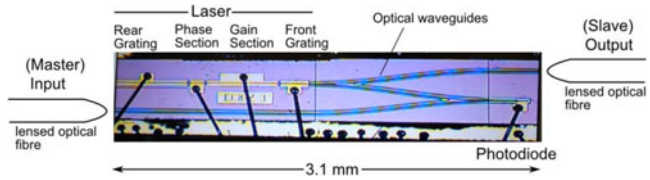

Fig. 1. Photonic integrated circuit containing DBR laser and photodiode.

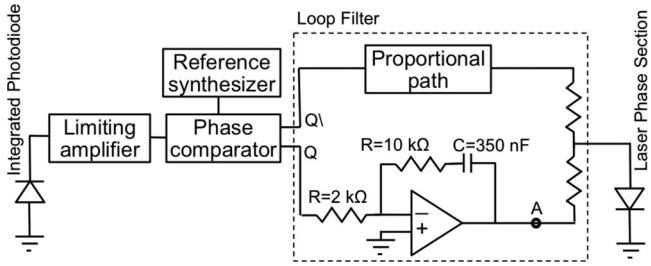

Fig. 2. Simplified block diagram of the OPLL feedback electronic circuit. Laser bias circuitry is not included.

In this paper we review the design and the performance of a monolithically integrated OPLL (see Section II). The most important parameters and design trade-offs of the OPLL, including a universal technique for OPLL gain (K) assessment, are described in Section III. The generation and the characteristics of a spectrally pure and tuneable microwave signal are included in Section IV followed in Section V by a discussion of the generation of sub-THz signals and the limitations to be overcome to achieve continuous tuneability.

II. The Optical Phase Lock Loop

The most general heterodyne OPLL is a negative feedback loop where the current controlled optical source (slave laser, SL) can be automatically phase synchronized (locked) to an optical input reference signal (master laser, ML) with the frequency offset corresponding to the external reference synthesizer frequency [8].

The single-OPLL system presented in this paper consists of a photonic integrated chip (PIC) and dedicated electronics for the laser's phase stabilisation. The InP-based monolithic PIC contains a broadly tuneable ($\sim$ 8 nm), buried distributed Bragg reflection (DBR) laser, a PIN photodiode, passive optical waveguides and Y-junction couplers and splitters used as interconnections. A microscope picture of the PIC is presented in Fig. 1. The PIC's fabrication process was previously described in detail in [14].

A. Feedback Electronics

The OPLL feedback electronics consist of a limiting amplifier and phase comparator followed by a two-path loop filter realised on a multilayer printed circuit board which contains commercially available 10 Gb/s emitter coupled logic and current mode logic integrated circuits. The simplified block diagram of the electronic board is presented in Fig. 2, and was previously extensively described in [15]. The beat signal from the integrated photodiode is amplified to the voltage level required by the logic circuits by a limiting amplifier, and its phase is compared against an external RF reference source using an XOR gate. The error signal from the XOR gate non-inverted (Q) and inverted $(Q\backslash)$ outputs is coupled into the integrating and the proportional path of the loop filter before being fed back into the laser's phase tuning section. The loop filter consists of two separated paths: a high-speed proportional path and slower integral paths. The former offers a short propagation delay ($<$1.8 ns) and a 3 dB open-loop bandwidth greater than 1 GHz for tracking fast changes. The integral path tracks a wider range of frequency changes, mostly caused by the laser thermal drift. The effect of the integrated path is limited up to $\sim$300 Hz, so although the OPLL was designed as type II, its response is dominated by the fast proportional loop and can be analysed as a first-order (Type I) loop. Due to the frequency responses of the components of the loop, the offset locking range (set by an external RF reference) was limited to 2–7 GHz [16].

B. Semiconductor Laser Performance

From the phase control system perspective, the laser could be seen as an oscillator with a current controllable frequency. The desired requirements placed on the loop oscillator, and therefore on the laser, are as follows: low phase noise (narrow linewidth), wide tuning range and tuning linearity, fast (wideband) modulation capability, low power consumption and small size suitable for photonic integration purposes. The DBR lasers monolithically integrated on the OPLL PIC fulfil most of these requirements; however the phase noise remains an outstanding issue. It is typical for the diode lasers to have a Lorentzian linewidth in the lower megahertz range [17]. The SL linewidth was measured, using the self-heterodyne technique, with a 5 km fibre delay line, to be 1.1 MHz (FWHM) [18]. Moreover the linewidth can be additionally broadened by the noise from power supplies used to bias the laser's sections, contributing to the measured 50 MHz FWHM linewidth of the heterodyne signal generated by photomixing two free running lasers (see Fig. 8).

The DBR consists of four separated sections, each with individual bias contacts. The coarse tuning mechanism of the laser is realised through current injection into the front and rear Bragg grating sections. In the operating system the phase error current is injected into the short phase section of the laser. The key parameter for the loop design is the laser tuning sensitivity, which reached 4.6 GHz/mA when measured on a discrete laser similar to that used in the OPLL. After assembly of feedback electronics the DC laser tuning sensitivity varied between 1.2 and 1.5 GHz/V, depending on the laser gain bias current. This was measured with respect to the voltage at the output of the integral path (see point A in Fig. 2), while the change of optical wavelength was measured using an optical spectra analyser (see Fig. 3).

It can be noticed that the laser's tuning sensitivity varies depending on the laser's gain current value. This characteristic implies that the laser may respond differently to the same value of the error current applied. This will cause the change in the loop gain and instantaneously in the loop bandwidth, thus influencing the quality of the lock.

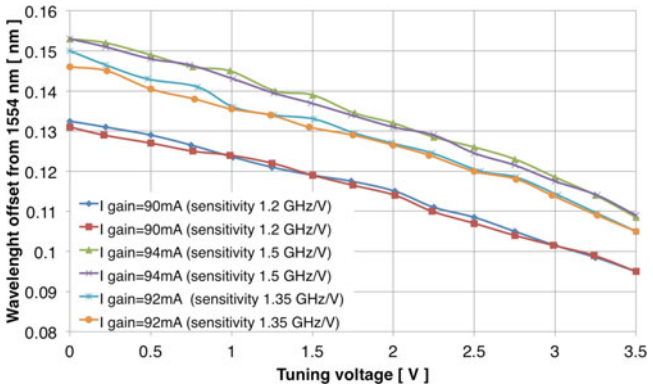

Fig. 3. Laser wavelength change as a function of tuning voltage (point A in Fig. 2).

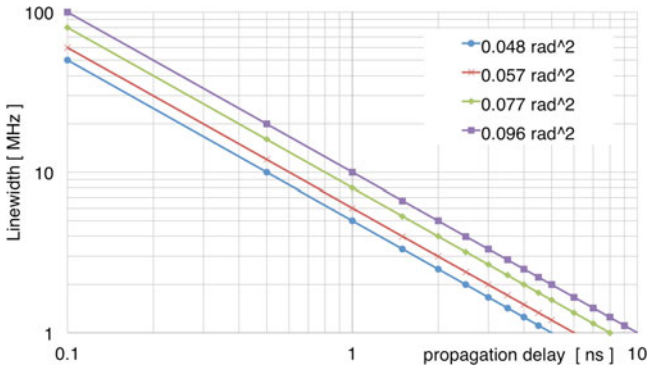

Fig. 4. Relation between lasers summed linewidth and delay in the loop for different phase error variances

C. Integrated Photodetector

A monolithically integrated PIN photodiode was included on the PIC to detect the beat note between the slave and master lasers; the device was 50 μm long and 7 μm wide. The design was based on a ridge waveguide and the same active material as the DBR lasers [14]. The photodiode –3 dB bandwidth was assessed to be approximately 12.5 GHz, which is higher than the frequency limit introduced by the electronic feedback board. The dark current of 10 μA was measured for applied bias voltage of -1.5 V. The photocurrent produced due to the integrated laser was approximately 500 μA when the DBR laser gain current was about 90 mA.

III. OPLL Parameters Analysis

The SL transfer function could be assumed to be as follows:

$$\frac{d\phi_{\mathrm{SL}}}{dt} = k_{\mathrm{SL}} i_e * h_{\mathrm{SL}} \tag{1}$$

where $k_{\mathrm{SL}}\left(\frac{\mathrm{rad}}{\frac{\mathrm{sec}}{\mathrm{mA}}}\right)$ and h_{SL} represent the SL sensitivity and impulse response, respectively, i_e is the error signal generated by the phase comparator, which is subsequently filtered by a low-pass filter and used to modulate the frequency of the SL. The effect of the loop propagation time delay and impulse responses of all the loop components will inevitably have an influence on the error signal, which is fed into the SL and which can be expressed as follows:

$$i_e = k_{\mathrm{LF}} k_{\mathrm{Mix}} K_{\mathrm{PD}} k_{\mathrm{amp}} \sin[(\omega_{\mathrm{RF}-}\omega_{\mathrm{SL}} + \omega_{\mathrm{ML}})t + \phi_{\mathrm{RF}-}\phi_{\mathrm{SL}} + \phi_{\mathrm{ML}}] * h_{\mathrm{LF}} * h_{\mathrm{Mix}} * h_{\mathrm{amp}} * \delta(t - \tau_d) \tag{2}$$

where

k_{LF}	loop filter gain;
k_{PD}	photodetector gain;
k_{Mix}	phase detector conversion efficiency;
k_{amp}	amplifier gain;
$\omega_{\mathrm{RF}} \cdot \varphi_{\mathrm{RF}}$	reference signal angular frequency and phase;
h_{LF}	loop filter impulse response;
h_{Mix}	mixer equivalent impulse response;
h_{amp}	amplifier response;
τ_d	loop propagation delay.

To simplify calculations, some of the loop components, such as the mixer, amplifier, photodetector, transmission lines and connectors, can be removed from the equations assuming they are constant over the frequency range of operation. Thus, the equations (1) and (2) are merged into

$$\frac{d\phi_{\mathrm{SL}}}{\mathrm{dt}} = 2\pi K \phi_{\mathrm{error}} * h_{\mathrm{LF}} * h_{\mathrm{SL}} * \delta(t - \tau_d) \tag{3}$$

where $\phi_{\mathrm{error}} = \phi_{\mathrm{RF}} - \phi_{\mathrm{SL}} + \phi_{\mathrm{ML}}$ represents the relative phase difference between SL and ML in reference to the external synthesizer (RF)

$$K = k_{\mathrm{LF}} k_{\mathrm{Mix}} k_{\mathrm{PD}} k_{\mathrm{amp}} k_{\mathrm{SL}} \tag{4}$$

is the overall gain in the loop.

From that simplified model one can identify the design trade-offs and assess the most critical loop parameters, such as gain and propagation delay. Both parameters are important as they can be used to predict loop bandwidth, lock-in range, hold-in range and the loop's ability to control the phase noise.

A. Propagation Delay and Laser Linewidth Trade-Off

The relation between an initial laser linewidth and the required propagation delay within the loop needs to be emphasised as these two factors influence the quality of the control system. Moreover the relation between these two parameters can be used as guidance to define whether the OPLL can operate in a stable locked condition.

In order to successfully phase lock an optical source with a relatively wide linewidth, a loop with a large bandwidth is required. Consequently, as the transit time of the error signal around the loop becomes important, it must be considered in the loop design and should be kept less than a fraction of the reciprocal of the loop natural frequency [19]. To ensure the required phase error variance or to avoid loop performance degradation, a compromise between laser linewidth, loop bandwidth and loop propagation delay must be found.

The relationship between the propagation delay and the sum of the ML and SL linewidths, for a type I loop with gain optimised to minimise the phase error variance, is inversely proportional, as illustrated in Fig. 4 for phase error variance ranging between 0.048 and 0.096 rad^2.

The first OPLL used to stabilise a semiconductor laser diode with 7.5 MHz linewidth was based on the homodyne phase locking [20]. The first packaged heterodyne OPLL, used to stabilise 6 MHz summed lasers linewidth and offering 40 ps delay, required very sensitive free space optics components [5]. Later, a hybrid integrated OPLL allowed a 1 MHz linewidth laser to be phase locked, despite a 10 mm path length between the laser and photodiodes, which made delay reduction difficult [8]. For the system described in section II, based on a measured summed linewidth of 2 MHz and a loop delay estimate of 1.8 ns, the calculated phase error variance (σ_{ph}^2) is 0.034 rad^2 and the loop noise bandwidth (B_n) is 232 MHz.

For these values, the mean time between cycle slips (T_{cs}), estimated using the formula [21]

$$T_{cs} = \frac{\pi}{4B_n} \exp\left(2/\sigma_{ph}^2\right) \tag{5}$$

is 4.02 $\times$ 10^{16} s, which corresponds to several decades mean time between cycle slips, suggesting that cycle slipping should not be an issue.

B. Gain

These values of the different parameters of the loop can be defined at the design stage of the OPLL development. However, to the best of our knowledge, measurement of the parameters of a fully assembled, operating OPLL system has not previously been reported.

In this paper we propose a technique which allows an experimental assessment of the gain in the operational system, feasible only if stable locking is achieved. In order to measure the gain (K), the single OPLL assembly presented in Fig. 7 was used. The loop operating conditions were changed by readjusting the SL gain current, while keeping the reference offset frequency fixed. The SL gain current was increased by 4 mA from the previous operational condition at 90 mA. This caused the loop gain to change, mainly due to changes in the SL tuning sensitivity as the bias current of the phase section changed to maintain the same locked frequency. The variation in the laser tuning sensitivity as a function of the laser DC tuning voltage is presented in Fig. 3. Thanks to the extensive hold-in range, the loop remained in the locked condition. As a consequence of the increasing loop gain, the secondary peaks became visible in the phase noise spectra. Instantaneously, the phase noise power at lower offset frequencies was increasingly reduced. To confirm these observations the calculated phase noise spectral density [22] for different values of gain (K) were calculated and are shown in Fig. 5.

Thereafter, the secondary peak power was measured with respect to the minimum phase noise power at small offset frequencies from the carrier. The measured relative power of the secondary peak is plotted against the offset frequency of the secondary peak in Fig. 6. As the loop gain increased, the frequency offset and relative peak power both increased. Further increase in the loop gain resulted in unstable locking and eventually a complete loss of lock. Calculations of the phase noise [23] for the measured laser linewidths and estimated loop propagation

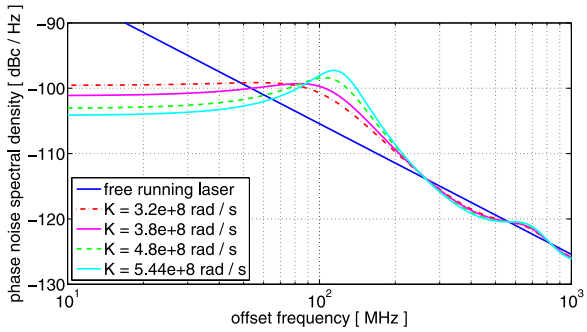

Fig. 5. Changes of the phase noise spectral density at low offset frequencies from the carrier for a range of different gains (K), calculated for the first order optical phase lock loop.

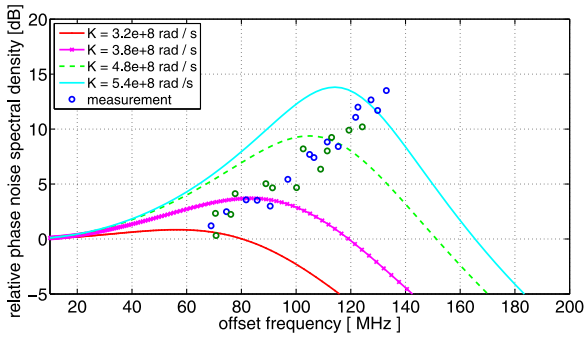

Fig. 6. Peak height of the phase noise spectral density for the first order optical phase lock loop.

delay of 1.8 ns allow assessing the range of the loop gain (K) to be between 3.2 $\times$ 10^8 and 5.44 $\times$ 10^8 rad/s.

It can be seen that the frequency offset of the measured peak is slightly higher than that predicted by the simulation. This could be explained by the fact that the frequency response of the loop components other than the loop filter was assumed to be uniform.

This result shows that the proposed gain assessment technique could be applied to different OPLL systems providing they are in a stable locked condition and are characterised by the extensive hold-in range.

IV. Experimental Results

The overall performance of the integrated OPLL PIC was assessed by heterodyning the master signal and SL output on a broad bandwidth (>50 GHz) photodiode connected to a high-performance electrical spectrum analyser. This approach reduced complexity and allowed the phase locked heterodyne signal to be observed directly on the spectrum analyser, without the need to use any down-conversion procedures [24].

The schematic of the experimental arrangement is presented in Fig. 7. The temperature of the PIC submount was controlled through a Peltier cooler. Two lensed fibres with a spot size diameter of 3 μm and the working distance of approximately 20 μm were aligned at the front and rear facet of the PIC. The input fibre was used to couple the reference signal into the buried optical waveguide and hence into the integrated photodetector. The

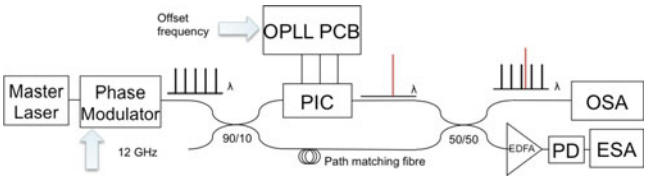

Fig. 7. Schematic of the measurement assembly

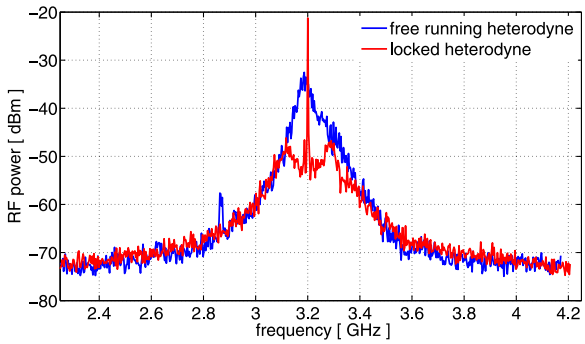

Fig. 8. Spectrum of the unlocked and locked signals at an offset of 3.2 GHz, detected on the integrated photodiode.

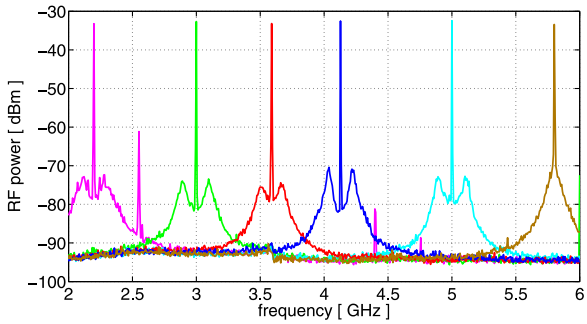

Fig. 9. Measured beat note spectra for different offset frequencies in range from 2 GHz to 6 GHz (RBW = 200 kHz, VBW = 10 kHz)

second fibre collected the output signal of the phase stabilised SL.

Depending on the experimental assembly the OPLL could be locked to a single frequency master laser or to an optical frequency comb generator (OFCG) [25].

The spectra for the free running and the offset phase locked heterodyne signal between the SL and the master are presented in Fig. 8.

An external cavity laser with a linewidth of 100 kHz was used as the master laser; the linewidth of the SL was measured to be 1.1 MHz (FWHM). The unlocked beat note exhibits a slow frequency drift over more than 500 MHz due to the variations of temperature. Once locked, the beat note exhibited a signal peak power improvement and the expected linewidth reduction up to the bandwidth to the OPLL.

Offset tuning of this monolithically integrated OPLL system across 4 GHz was achieved by changing the reference synthesizer frequency between 2 and 6 GHz (see Fig. 9). To acquire locking, the frequency difference between the slave and the master laser must be close to the reference frequency and therefore needs to be manually set. This can be achieved by changing

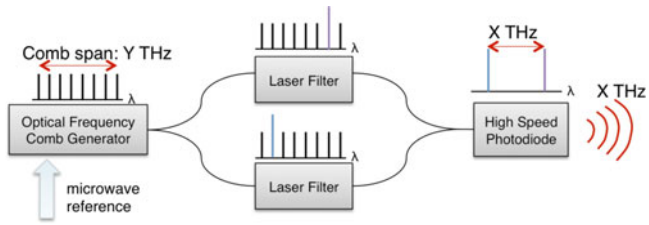

Fig. 10. Scheme of the photonic oscillator based on the dual optical filter

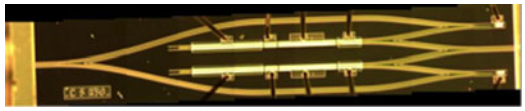

Fig. 11. Dual-OPLL photonic integrated circuit containing DBR lasers and photodiodes

the laser front and rear grating currents, thus tuning the laser wavelength.

Moreover, the system is capable of acquiring stable lock regardless of which of the two lasers, master or slave, has the longer wavelength [25]. This means that the SL can be locked to both sides of any of the comb line of interest.

Fig. 9 also demonstrates changes to the loop gain across the tuning range, as reflected in the magnitude of the side lobes (see Section III). Across the tuning range a FWHM linewidth of less than 10 Hz (measurement limited) was measured.

The single side-band phase noise performance of less than -80 dBc/Hz at offsets above 10 kHz of the heterodyne between the slave and the master laser was achieved [16], [26]. The phase error variance of the generated heterodyne signal, measured in bandwidth from 1 kHz to 10 GHz, was between 0.038 and 0.22 rad^2 (depending on the loop gain), as presented in [26].

V. Dual OPLL, for Frequency Generation

One potential use of the OPLL PIC is to develop a dual arm circuit for frequency generation in combination with an OFCG to enable high-performance millimetre-wave and THz sources as represented in Fig. 10. The source, based on the photonic synthesis, would consist of i) a broad span OFCG to provide a reference in the form of a phase-correlated train of optical frequencies, ii) an ultrafast photodiode to convert the heterodyne signal from optical into electrical domain [27] and iii) two OPLLs used as a very narrow bandwidth ($<$1 GHz) optical filters which can amplify and frequency offset the two selected comb lines of interest.

A single chip can integrate all photonic components required to build two OPLL-based optical filters, such as two DBR lasers, two PIN photodiodes and optical waveguides. A photograph of such a PIC is presented in Fig. 11. The monolithic integration approach significantly reduces the overall size of the system, but also makes it more resistant to environmental changes. For instance, both lasers are equally affected by temperature changes, which improves the long-term frequency stability and linewidth of the heterodyne signal.

Higher frequency, spectrally pure signals can be generated by increasing the wavelength spacing between two DBR lasers

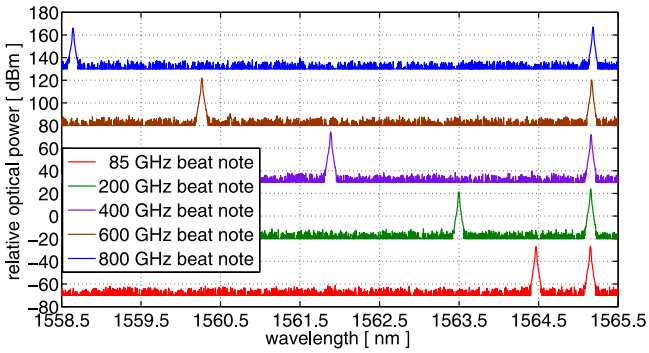

Fig. 12. Optical spectra of two free running widely tuneable DBR lasers

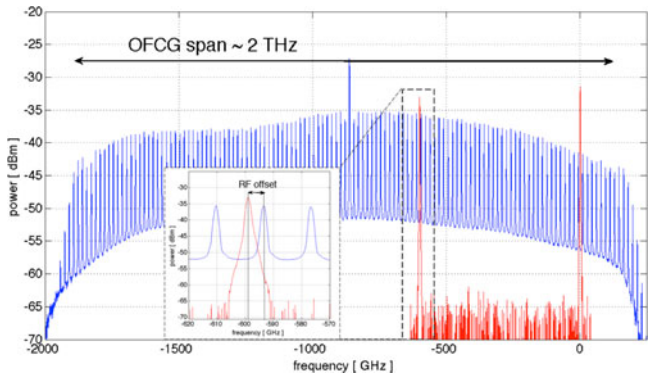

Fig. 13. Measured optical spectra of the comb (blue line) and two tuneable DBR slave lasers integrated on singe PIC (red line).

and phase locking each of them to the corresponding comb lines. This ensures that both SLs will simultaneously follow any phase change (within the locking range) of the reference OFCG, while the spacing between the SLs will remain constant, ensuring generation of absolute frequency. Both DBR lasers offer a tuning range of 7–9 nm, which is sufficient to generate the beat note of any frequency between the microwave and THz range through photomixing. The tuning capabilities of the DBR laser are shown in Fig. 12.

For the purposes of this experiment a broad span OFCG would be required, for instance, a recirculating amplified fibre loop with a phase modulator [28], which can generate comb with the span of up to 2 THz, would be suitable.

Measured optical spectra of the two monolithically integrated DBR lasers spaced by 800 GHz together with 2 THz span optical comb are presented in Fig. 13.

The photocurrent from the integrated laser is approximately 500 μA when the laser is operating at 70 mA gain current. However the photocurrent associated with the coupled OFCG signal was below 15 μA, when the optical reference signal was amplified up to 22 dBm before being coupled into the dual-OPLL PIC. This suggests either high propagation losses in the optical waveguides or low coupling efficiency at the facet. The OPLL electronics require at least -40 dBm of RF power from the integrated PD to achieve stable locked operation. This requirement was barely met thus limiting the operation and locking ability of the system. However a demonstration at the optimum offset frequency, where sufficient loop gain was obtained, was done

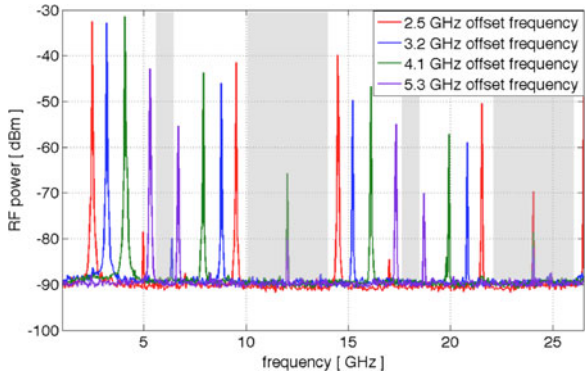

Fig. 14. Heterodyne signals between OFCG and DBR lasers at different offset locking frequencies. The grey area indicates the restricted frequencies which cannot be generated by the photonic source based on a single OPLL.

for signal frequencies up to 50 GHz and high purity signal was demonstrated [14].

A. *Tuneability of the High Frequency Signal Source*

As expected, the continuous tuneability range of the system is limited by the bandwidth of the components of the loop. For the OPLL described here this was the amplifier and the phase comparator. With higher performance electronics, OPLLs with higher frequency offsets of up to 18 GHz [29] and, more recently, of up to 9 GHz [30] were also reported. However for the dual arm-OPLL in which SLs are locked to the comb lines, the influence of the beat with adjacent comb lines onto the locked OPLL within the loop bandwidth must be taken into account.

One would expect that when the difference of offsets between the slave and the two adjacent comb lines falls within the loop bandwidth, instabilities will occur and will prevent the acquisition of lock at offset frequencies close to half of the frequency spacing between the comb lines. Therefore spacing between the comb lines should be selected in such a way as to be equal or greater than

$$F_{\mathrm{comb}} \geq 2 \times f_{\mathrm{offset}} + F_{\mathrm{BW}} \tag{6}$$

where f_{offset} should be considered as the highest offset locking frequency in GHz, and F_{BW} is an open loop bandwidth of the loop filter. This was demonstrated in [25] where the OPLL system was locked at the highest offset of 5.3 GHz for the comb lines spaced by 12 GHz, while the open loop bandwith of the loop filter is greater than 1 GHz [26].

Using the system in Fig. 7, beat notes can be generated by photomixing the OFCG and the SL locked to one of the comb lines at different offset frequencies. The spectra of these beat notes for the range of offset frequencies are presented in Fig. 14.

The part of the spectrum shown as a grey area in Fig. 14 cannot be easily accessed when a single OPLL with 4 GHz tuneability between the comb lines and a OFCG with 12 GHz comb line spacing are used. It can also be noted that a set of unwanted beat notes with other comb lines appear as expected on the spectrum. This suggests that two aspects would need to be addressed before a fully operational, broadly tuneable and spectrally pure photonic source for mm-wave or THz generation based on the

OPLL can be achieved: all unwanted frequencies must be suppressed, and, second, access to the frequencies between the comb lines must be improved, i.e. the tuneability should be further increased. Both limitations can be easily compensated by implementing a second OPLL with identical performances. The dual OPLL-based system increases the tuneability by allowing access to any desired frequency between the comb lines; it also suppresses all unwanted photomixing products.

It must be noted that even though the input to the OPLL may contain all OFCG lines, the output of the discussed system is only the SL wavelength. This means that the OPLL can be considered as a high quality active optical filter with a very narrow bandwidth and gain. Such a dual OPLL, phase locked to an OFCG would therefore create a broadly tuneable, photonic source for the mm-wave and THz generation with the highest generated frequency being defined by either the comb span or the tuning range of the lasers.

VI. Conclusion

The characteristics and properties of a monolithically integrated OPLL system, such as tuneability and long-term frequency locking were demonstrated. A heterodyne signal with linewidth in range of tens of Hz was generated. The relation between the loop delay and the summed laser linewidths, which determines the stable bandwidth of the OPLL, was explained. A technique to evaluate the gain of the OPLL was proposed, analysed and experimentally verified. The potential for dual OPLL continuously tuneable frequency sources was discussed and a demonstration of such a source was done for frequency below 50 GHz while the tuning of the lasers on chip would potentially allow for frequency generation up to 1.8 THz.

Acknowledgment

The authors would like to thank their collaborators at the University of Ljubljana and the Centre for Integrated Photonics for their help in developing the devices and circuits, as well as their contribution in the framework of the PORTRAIT (UK EPSRC) and IPHOBAC (EU) projects.

References

[1] A. J. Seeds, "Microwave photonics," *IEEE Trans. Microw. Theory Tech.*, vol. 50, no. 3, pp. 877–887, Mar. 2002.

[2] J. Capmany and D. Novak, "Microwave photonics combines two worlds," *Nature Photon.*, vol. 1, pp. 319–330, 2007.

[3] B. Vidal, T. Nagatsuma, N. J. Gomes, and T. E. Darcie, "Photonic technologies for millimeter- and submillimeter-wave signals," *Adv. Opt. Technol.*, vol. 2012, pp. 1–18, 2012.

[4] A. J. Seeds and K. J. Williams, "Microwave photonics," *J. Lightw. Technol.*, vol. 24, no. 12, pp. 4628–4641, Dec. 2006.

[5] L. N. Langley, M. D. Elkin, C. Edge, M. J. Wale, U. Gliese, X. Huang, and A. J. Seeds, "Packaged semiconductor laser optical phase-locked loop (OPLL) for photonic generation, processing and transmission of microwave signals," *IEEE Trans. Microw. Theory Tech.*, vol. 47, no. 7, pp. 1257–1264, Jul. 1999.

[6] S. Fukushima, C. Silva, Y. Muramoto, and A. J. Seeds, "Optoelectronic millimeter-wave synthesis using an optical frequency comb generator, optically injection locked lasers, and a unitraveling-carrier photodiode," *J. Lightw. Technol.*, vol. 21, no. 12, pp. 3043–3051, Dec. 2003.

[7] A. C. Bordonalli, C. Walton, and A. J. Seeds, "High-performance phase locking of wide linewidth semiconductor lasers by combined use of optical injection locking and optical phase-lock loop," *J. Lightw. Technol.*, vol. 17, no. 2, pp. 328–342, Feb. 1999.

[8] R. J. Steed, L. Ponnampalam, M. J. Fice, C. C. Renaud, D. C. Rogers, D. G. Moodie, G. D. Maxwell, I. F. Lealman, M. J. Robertson, L. Pavlovic, N. Luka, V. Matjaz, and A. J. Seeds, "Hybrid integrated optical phase-lock loops for photonic terahertz sources," *IEEE J. Sel. Topics Quantum Electron.*, vol. 17, no. 1, pp. 210–217, Jan./Feb. 2011.

[9] S. Ristic, A. Bhardwaj, M. J. Rodwell, L. A. Coldren, and L. A. Johansson, "An optical phase-locked loop photonic integrated circuit," *J. Lightw. Technol.*, vol. 28, no. 4, pp. 526–538, Feb. 2010.

[10] M. J. Fice, A. Chiuchiarelli, E. Ciaramella, and A. J. Seeds, "Homodyne coherent optical receiver using an optical injection phase-lock loop," *J. Lightw. Technol.*, vol. 29, no. 8, pp. 1152–1164, Apr. 2011.

[11] T. Nagatsuma, "Generating millimeter and terahertz waves,". (2009, Jun.). *IEEE Microw. Mag.*, vol. 10, no. 4, pp. 64–74, 2009.

[12] L. A. Coldren, "Photonic integrated circuits for microwave photonics," in *Proc. IEEE Top. Meeting Microw. Photon.*, Oct. 2010, pp. 1–4.

[13] M. Smit, X. Leijtens, E. Bente, J. Van der Tol, H. Ambrosius, D. Robbins, M. Wale, N. Grote, and M. Schell, "Generic foundry model for InP-based photonics," *IET Optoelectron.*, vol. 5, no. 5, pp. 187–194, Oct. 2011.

[14] L. Ponnampalam, M. Fice, F. Pozzi, C. Renaud, D. Rogers, I. F. Lealman, D. G. Moodie, P. J. Cannard, C. Lynch, L. Johnston, M. J. Robertson, R. Cronin, L. Pavlovic, L. Naglic, M. Vidmar, and A. Seeds, "Monolithically integrated photonic heterodyne system," *J. Lightw. Technol.*, vol. 29, no. 15, pp. 2229–2234, Aug. 2011.

[15] L. Naglic, L. Pavlovic, B. Batagelj, and M. Vidmar, "Improved phase detector for electro-optical phase-locked loops," *Electron. Lett.*, vol. 44, no. 12, pp. 44–45, 2008.

[16] K. Balakier, M. J. Fice, L. Ponnampalam, C. C. Renaud, and A. J. Seeds, "Tuneable monolithically integrated photonic THz heterodyne system," in *Proc. IEEE Int. Top. Meeting Microw. Photon.*, Sep. 2012, pp. 286–289.

[17] M. C. Amann and J. Buus, *Tuneable Laser Diodes*. Norwood, MA, USA: Artech House, 1998.

[18] A. J. Seeds, F. Pozzi, C. C. Renaud, M. J. Fice, L. Ponnampalam, D. C. Rogers, I. F. Lealman, and R. Gwilliam, "Microwave photonics: Opportunities for photonic integration," in *Proc. Eur. Conf. Integr. Opt.*, 2008, pp. 123–132.

[19] M. A. Grant, W. C. Michie, and M. J. Fletcher, "The performance of optical phase-locked loops in the presence of nonnegligible loop propagation delay," *J. Lightw. Technol.*, vol. LT-5, no. 4, pp. 592–597, Apr. 1987.

[20] M. Kourogi, C.-H. Shin, and M. Ohtsu, "A 134 MHz bandwidth homodyne optical phase-locked-loop of semiconductor laser diodes," *IEEE Photon. Technol. Lett.*, vol. 3, no. 3, pp. 270–272, Mar. 1991.

[21] F. M. Gardner, *Phaselock Techniques*. Oxford, U.K.: Wiley, 2005.

[22] R. T. Ramos and A. J. Seeds, "Comparison between first-order and second-order optical phase-lock loops," *IEEE Microw. Guided Wave Lett.*, vol. 4, no. 1, pp. 7–9, Jan. 1994.

[23] R. T. Ramos and A. J. Seeds, "Delay, linewidth and bandwidth limitations in optical phase-locked loop design," *Electron. Lett.*, vol. 3, pp. 389–391, 1990.

[24] J. Borner, G. Pillet, L. Morvan, D. Dolfi, K. Balakier, and C. Renaud, "Optical demodulation of THz signals," in *Proc. IEEE Photon. Conf.*, Sep. 2013, vol. 5, pp. 209–210.

[25] K. Balakier, M. J. Fice, L. Ponnampalam, A. J. Seeds, and C. C. Renaud, "Tuneability of monolithically integrated optical phase lock loop for THz generation," in *Proc. IEEE Int. Top. Meeting Microw. Photon.*, 2013, pp. 182–185.

[26] R. J. Steed, F. Pozzi, M. Fice, C. Renaud, D. C. Rogers, I. F. Lealman, D. G. Moodie, P. J. Cannard, C. Lynch, L. Johnston, M. J. Robertson, R. Cronin, L. Pavlovic, L. Naglic, M. Vidmar, and A. J. Seeds, "Monolithically integrated heterodyne optical phase-lock loop with RF XOR phase detector," *Opt. Exp.*, vol. 19, no. 21, pp. 20048–20053, Oct. 2011.

[27] E. Rouvalis, C. C. Renaud, D. G. Moodie, M. J. Robertson, and A. J. Seeds, "Continuous wave terahertz generation from ultra-fast InP-Based photodiodes," *IEEE Trans. Microw. Theory Tech.*, vol. 60, no. 3, pp. 509–517, Mar. 2012.

[28] S. Bennett, B. Cai, E. Burr, O. Gough, and A. J. Seeds, "1.8-THz bandwidth, zero-frequency error, tunable optical comb generator for DWDM applications," *IEEE Photon. Technol. Lett.*, vol. 11, no. 5, pp. 551–553, May 1999.

[29] U. Gliese, T. Nielsen, M. Bruun, E. L. Christensen, and K. E. Stubkjaer, "A 3-18 GHz microwave signal generator based on optical phase locked semiconductor DFB lasers," in *Proc. Lasers Electro-Opt. Soc.*, 1993, pp. 5–6.

[30] M. Lu, H. Park, E. Bloch, A. Sivananthan, A. Bhardwaj, Z. Griffith, L. A. Johansson, M. J. Rodwell, and L. A. Coldren, "Highly integrated optical heterodyne phase-locked loop with phase / frequency detection," *Opt. Exp.*, vol. 20, no. 9, pp. 1090–1092, 2012.

Katarzyna Balakier received the M.Sc. degree in electronics and telecommunications with specialisation in optoelectronics from Białystok Technical University, Białystok, Poland, in 2006. She is currently working toward the Ph.D. degree at the University College London, London, U.K.

She worked as an Engineer for LG Electronics between 2006 and 2007. In 2007, she moved to Madrid, Spain to join Sener Ingenieria y Sistemas, where she worked in the Aerospace Division on development of metrology and spectroscopy systems for space applications. In 2010, she was appointed as a Marie Curie Research Fellow with the Ultra-fast Photonics Group, University College London. Her research interests include photonic integrated circuits for microwave and THz signals generation as well as phase stabilization techniques.

Martyn J. Fice (S'86–M'87) received the B.A. degree in electrical sciences and the Ph.D. degree in microelectronics from the University of Cambridge, Cambridge, U.K., in 1984 and 1989, respectively.

In 1989, he joined STC Technology Laboratories, Harlow, U.K. (later acquired by Nortel), where he was engaged for several years in the design and development of InP-based semiconductor lasers for undersea optical systems and other applications. Subsequent work at Nortel involved research into various aspects of optical communications systems and networks, including wavelength-division multiplexing, all-optical wavelength conversion, optical regeneration, and optical packet switching. Since 2005, he has been a Senior Research Fellow with the Photonics Group, Department of Electronic and Electrical Engineering, University College London, London, U.K. His current research interests include millimeter and THz wave generation and detection, optical phase locking, coherent optical detection, and optical transmission systems.

Dr. Fice is a Member of the Institution of Engineering and Technology and a Chartered Engineer.

Lalitha Ponnampalam received the B.Eng. degree from the University College London, London, U.K., the M.S.E.E. degree from the School of Optics, University of Central Florida, Orlando, FL, USA, and the Ph.D. degree from the University of Cambridge, Cambridge, U.K.

She is currently working as a Research Fellow in the Ultrafast Photonics Group, University College London, London, U.K., having interests in tuneable lasers, terahertz signal generation, and integrated optics. She previously worked on the design and development of widely tuneable lasers at Bookham Technology, Caswell, which became part of Oclaro Inc.

Dr. Ponnampalam is a Member of the Institute of Engineering and Technology.

Alwyn J. Seeds received the Ph.D. and D.Sc. degrees from the University of London, London, U.K.

After working as a Staff Member at MIT Lincoln Laboratory, he moved to University College London where he is currently a Professor of opto-electronics and Head of the Department of Electronic and Electrical Engineering. He has published more than 400 papers and filed some 15 patents on microwave and opto-electronic devices and their systems applications.

Prof. Seeds has been elected a Fellow of the Royal Academy of Engineering (UK) and an IEEE Fellow (USA). He has served as Vice-President for Technical Affairs of the IEEE Photonics Society (USA).

Cyril C. Renaud received the degree in engineering from the Ecole Supérieure d'Optique, Orsay, France, and the Diplôme d'Etudes Approfondies in Optics and Photonics from the University Paris XI, Orsay, France, in 1996. He received the Ph.D. degree for the work on diode pumped high-power ytterbium-doped fibre-lasers, with particular interest on Q-switched system and 980-nm generation from the Optoelectronics Research Centre, University of Southampton, Southampton, U.K., in 2001. In 1998, he spent one year as a project engineer with Sfim-ODS, working on the development of microchips lasers and portable range finders.

He is currently a Senior Lecturer at the University College London, London, U.K., and the UCL Site Director for the UCL/Cambridge Doctoral Training Centre in Integrated Photonic and Electronic Systems. His current research interests include optoelectronic devices and systems. It also include works on uncooled WDM sources, agile tuneable laser diode, and monolithic optical frequency comb generator using Quantum Confined Stark Effect, high-frequency photodetectors (UTC, travelling wave), photonic integration, and optical frequency generation systems in the optical and millimetre wave domains (DWDM, THZ). His work has led to more than 80 publications in international peer reviewed journals and conferences and three patents.